2D Tomographic velocity model building in tilted transversely isotropic media

Fan Jiang, Hua-wei Zhou, Zhi-hui Zou and Hui Liu, Texas Tech University*

Summary

The presence of tilted transverse isotropy (TTI) is a good approximation of the velocity structure for many dipping sand and shale strata and fractured carbonates. We evaluate here the effectiveness of tomographic inversion for 2D models consisting of several thickness-varying layers. Each model layer has a set of constant TTI parameters, the two Thomsen's parameters, the tilted angle of the symmetry axis, and the velocity along the axis. Several synthetic tests indicate that some combinations of the above TTI parameters plus the layer thickness are invertible using first-arrival traveltimes. Our tests show that error in estimating the tilted angle and layer thickness may lead to significant error in estimating the Thomsen's parameters. Hence it is erroneous to estimate Thomsen's parameters assuming a vertical symmetry axis in TTI media. A general workflow for TTI velocity model building is proposed and to be tested with further studies.

Introduction

Seismic anisotropy, the variation of the speed of seismic waves as a function of traveling direction, is caused by alignments of mineral crystals, fractures, and thin layers of alternative velocities. When sedimentation and tectonic processes produce dip and thickness variations in rock layers, their velocity structures may be approximated as TTI media. The symmetry axis of sedimentary strata with a short depositional history is usually assumed to be vertical and for old strata that have undergone deformation the symmetry axes trend to be normal to bedding (Hornby et al., 1994; Thomsen, 1995; Sayers, 2005). In thrust belts such as in the Canadian foothills (Charles et al., 2008), reservoir are overlain by thick sequences of dipping sandstone and shale layers which generate a tilted symmetry axis. The tilted angle of symmetry makes it more challenging to estimate the anisotropic parameters for TTI media than the cases of VTI (vertical transverse isotropy) when the symmetry axis is vertical, or HTI (horizontal transverse isotropy) when the symmetry axis is horizontal.

Most methods of analyzing seismic anisotropy focus on the time domain or data space analysis of surface reflection data (Grechka et al., 2001; Behera and Tsvankin, 2009). Residual moveout analysis of common image gathers is expected to be robust in handling common types of seismic anisotropy. However, how to reliably estimate anisotropic parameters of TTI media in depth domain or model space is still difficult, even if the tilted symmetry axis to be known. To reliably obtain Thomsen's δ parameter (Thomsen, 1986), for instance, the well control is needed. Large offsets are required to extract Thomsen's ε parameter. Some studies showed that fault plane reflection energy that intersects sedimentary reflectors may be helpful to estimate anisotropic parameters (Ball, 1995). Some recently workers (Zhou et al., 2004; Charles et al., 2008; Koren et al., 2008; Zhou et al., 2008) have focused on depth domain estimation of anisotropic parameters. However, it is challenging to solve all TTI parameters simultaneously without a priori information.

In this paper, we extended a layer tomography method (Zhou, 2006) to invert for TTI parameters as well as thickness-varying interface geometry using first arrivals. We use 2D synthetic tests to evaluate the ability to estimate the Thomsen's parameters, the tilted angle of the symmetry axis and layer velocity and geometry for crosswell and VSP acquisition geometries.

Methodology

To calculate P-wave traveltime in TTI media, we extend Sena's equation (1991) to:

$$t = \int L * (sw_{p0} * \sqrt{1 - 2\delta \sin^2(\theta - \varphi) + 2(\delta - \varepsilon)\sin^4(\theta - \varphi)}) \qquad (1)$$

where t and L are the traveltime and distance between two ray tracing nodes. sw_{p0} is the P-wave slowness along the symmetry axis, or axial slowness, ε and δ are Thomsen's parameters, and the group angle (θ-φ) is shown in Figure 1.

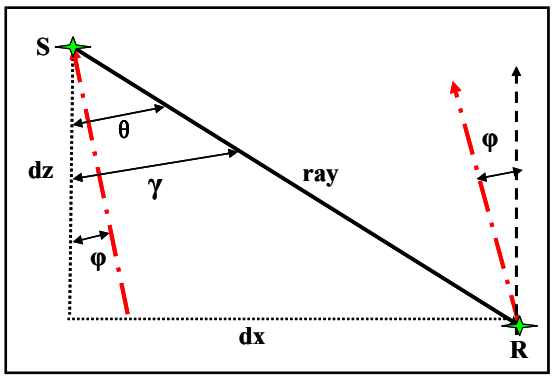

Figure 1: A sketch to illustrate TTI model. Variable φ is the tilted angle between vertical axis (dash line) and tilted symmetry axis (long dash dot line), θ is the angle between vertical axis and ray path (solid line), γ is the ray incident angle, or group angle (θ-φ). The variables dx and dz can be locally determined based on known ray tracing nodes.

Figure 2 shows the P-wave wavefronts generated by equation (1) implemented in anisotropic ray tracing in arbitrarily TTI media.

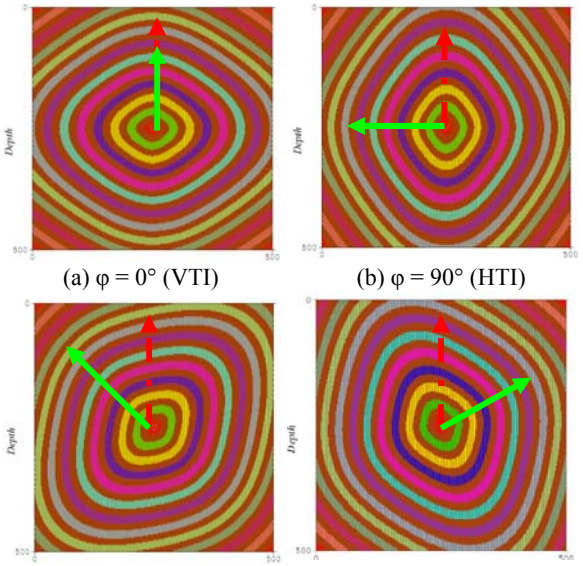

(a) φ = 0° (VTI) (b) φ = 90° (HTI)

(c) φ = 45° (d) φ = -67°

Figure 2: The P-wave wavefronts in TI media with the different tilted angle φ. (a) φ=0° (VTI) (b) φ=90° (HTI) (c) φ=45° (d) φ=-67°. Here sw_{p0}=1s/km, ε=0.18, δ=-0.15. Red dash line denotes the vertical axis, green solid line represents the direction of tilted symmetry axis.

By taking the first derivative of equation (1) with TTI parameters, the analytical kernel expressions can be proposed as:

$$\frac{dt}{d(sw_{p0})} = L * (1 - 2\delta\sin^2\gamma + 2(\delta - \varepsilon)\sin^4\gamma)^{1/2}$$

$$\frac{dt}{d\delta} = \frac{L * sw_{p0} * \left(\sin^4\gamma - \sin^2\gamma\right)}{\sqrt{1 - 2\delta\sin^2\gamma + 2\left(\delta - \varepsilon\right)\sin^4\gamma}}$$

$$\frac{dt}{d\varepsilon} = \frac{-(L * sw_{p0} * \sin^4\gamma)}{\sqrt{1 - 2\delta\sin^2\gamma + 2\left(\delta - \varepsilon\right)\sin^4\gamma}} \qquad (2a)$$

The sine function of the tilted angle can be expressed analytically as equation (2a). The analytical kernel of the sine function for a tilted angle is derived as:

$$\frac{dt}{d(\sin\varphi)} = L * sw_{p0} * \frac{\left[\begin{array}{l} 2\delta\sin\gamma(\sin\theta tg\varphi + \cos\theta\cos\varphi) + \\ 4(\varepsilon - \delta)\sin^3\gamma(\sin\theta tg\varphi + \cos\theta\cos\varphi) \end{array}\right]}{\sqrt{1 - 2\delta\sin^2\gamma + 2(\delta - \varepsilon)\sin^4\gamma}} \qquad (2b)$$

The comparison of analytical kernels verse numerical kernels in VTI media are analyzed in Figure 3. It is apparent that at the same group angle, the sensitivity of each TTI parameter can be quite different, e.g., ε is more depend on the ray paths in the horizontal direction or group angle close to 90° while δ is more affected by the raypaths with 45° dipping direction. It implies that such ray illuminations provide different resolutions when different acquisition geometries are concerned.

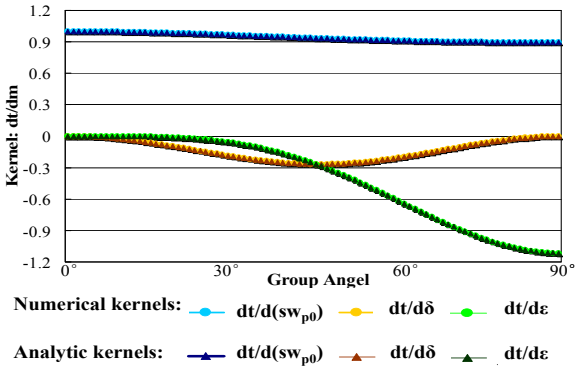

Figure 3: The comparisons between the analytical kernels denoted by triangles and numerical kernels denoted by circles. Here sw_{p0}=1s/km, ε=0.1, δ=0.15. Each numerical kernel is finite difference value by perturbing the corresponding parameter by 5%.

Synthetic test 1: VSP acquisition

The first example shows a tomographic inversion for the interface geometry and anisotropic parameters ε and δ for a walkaway VSP. The given parameters for the three model layers are the P-wave axial velocities of 2.0, 2.5, 3.0 km/s for the top to the bottom layers and the tilted angles of 10°, -10°, 1° for the symmetry axes of these layers. We used noise-free data to see how accurately the parameters can be obtained with poor initial guesses of the inversion parameters, ε and δ of three layers and geometry of the two model interfaces. Figure 4 illustrates that these TTI parameters can be well resolved by the new method under ideal situation. When ray coverage is better, the results are more accurate. The resultant features are consistent with the sensitivity behaviors of the TTI parameters. The solution error for each inversion parameters is defined as:

$$\text{Solution error} = \left|\frac{\text{True model value - Inverted value}}{\text{Range of the inversion parameter}}\right| \qquad (3)$$

In this paper, we assign a range of -20% to +20% for both ε and δ, which means the denominator in equation (3) is 0.4 for ε and δ. The range of velocity is from 1 to 4 km/s, and

the range of the tilted angle is from -50° to 50°. Figure 5 shows the solution errors for ε and δ as functions of the inversion iteration for this synthetic test.

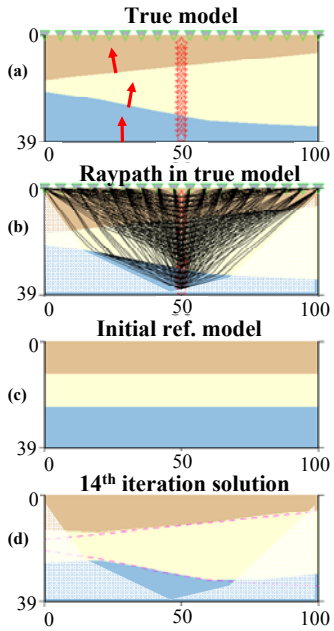

	True model	
	ε	δ
Layer1	0.15	0.10
Layer2	0.10	0.04
Layer3	0.14	0.15

	Ref. model	
	ε	δ
Layer1	0.0	0.0
Layer2	0.0	0.0
Layer3	0.0	0.0

	14th iteration	
	ε	δ
Layer1	0.150	0.100
Layer2	0.093	0.038
Layer3	0.134	0.135

Figure 4: 2D TTI VSP test. The red arrow in (a) denotes the tilted angle. The triangles represent source locations, and the stars denote geophone positions. Red numbers in right panel show the inverted parameters. The purple dash line in (d) indicates the true interface geometry. In panels (b) and (d), the region outside ray coverage is lightened.

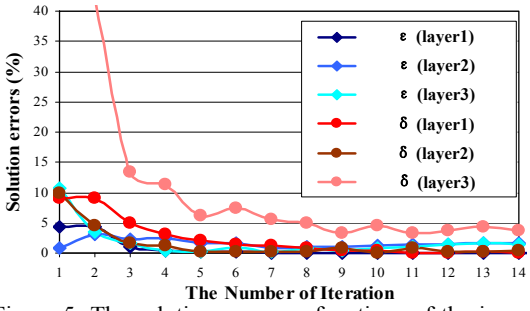

Figure 5: The solution errors as functions of the inversion iteration.

The inherent challenge of velocity modeling is the uncertainty of parameter estimation. TTI anisotropy is dominated in the tilted direction of primary thrusting, but counter thrusting and other minor deformation may reoriented or disrupt the effective symmetry axis. We analyze a test to invert for ε and δ by VTI assumption using the recorded TTI data from anisotropic ray tracing (Figure 4b). The given parameters are the interface geometries and P-wave axial velocity discussed in previous test. The tilted angles are considered as noises in data space. Table 1 shows the results where red number denotes the inverted parameter.

Table 1: VSP inversion test with noise.

	True mode (φ=10°; -10°; 1°)			Inversion result (φ = 0°; 0°; 0°)	
	ε	δ		ε	δ
Layer1	0.15	0.10		0.141	0.077
Layer2	0.10	0.04		0.098	0.046
Layer1	0.14	0.15		0.130	0.181

In this noise-contaminated test, ε can be better estimated than δ partly because δ is only sensitive when raypath direction is around 45° (Figure 3). However, this test demonstrates that the assumption of VTI in TTI media will degrade the quality of the parameter estimation. In this case, the error for ε is about 1.75% and the error for δ is about 5%.

Synthetic test 2: crosswell acquisition

Crosswell tomography can provide wide ray angle coverage for detecting anisotropy. We further show a crosswell tomographic inversion for the interface geometry, ε and the tilted angle φ (Figure 6). We experiment two inversions with different δ assumptions to test the robustness of our approach. In inversion I (Figure 6c), δ is assumed to be correct value in each layer, however in inversion II (Figure 6d), δ is assumed to be zero in each layer and is considered as noise in data space.

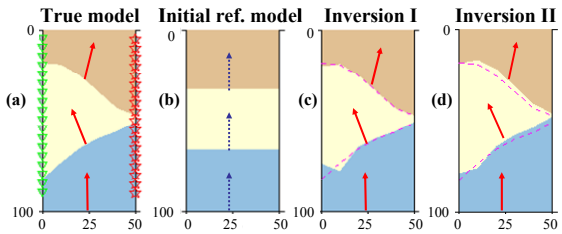

	True model			Inversion I		Inversion II	
	ε	φ	δ	ε	φ	ε	φ
Layer1	0.15	-14°	0.10	0.15	-14.079°	0.151	-12.559°
Layer2	0.10	22°	0.04	0.101	21.233°	0.095	26.584°
Layer3	0.14	1°	0.15	0.134	1.492°	0.156	-0.71°

Figure 6: 2D TTI crosswell test. (a) True model; (b) Reference model; (c) The result of inversion I with δ of 0.1, 0.04, 0.15 in each layer; (d) The result of inversion II with δ of 0.0, 0.0, 0.0 in each layer. Red arrows represent true symmetry axes in (a) and inverted symmetry axes in (b) and (d). Blue arrows denote the initial vertical symmetry axes.

Both inversions show good approximations. Inversion I is well resolved with the average solution errors of 0.58% for ε and 0.45% for tilted angle φ. The average solution errors for inversion II are 1.8% for ε and 2.58% for φ. Those inversions illustrate that even without δ information, other TTI parameters, such as interface geometry, ε or tilted angle φ, still can be recovered properly. The parameter δ can be recovered by re-applying tomographic inversion or moveout analysis.

Synthetic test 3: The influence of the tilted angle and the layer thickness on the parameter estimation

P-wave kinematic TTI signatures can be considered by P-wave axial velocity, interface geometry, Thomsen parameter ε and δ and tilted angle φ of symmetry axis. In many studies (Vestrum et al., 1999; Zhou et al., 2004; Behera and Tsvankin, 2009), the symmetry axis is assumed to be vertical or normal to bedding. Although those assumptions reduce the number of independent parameters, they will degrade the quality of the parameter estimation. To quantify the dependence of errors in parameter estimation, we repeated tomographic inversion for P-wave axial velocity, ε and δ with different assumptions of the tilted angles for the symmetry axes. The true model is same with Figure (4a) with the tilted angle of 10°, -10°, 0° for the symmetry axes from the top to the bottom layer. The tilted angle φ of first two layers will be rotated by 1° toward vertical axis at each test. At the eleventh test, the tilted angles are 0° in all three layers which become VTI media. Figure 7 shows the influence of the tilted angle for the symmetry axis on the accuracy of the parameter estimation.

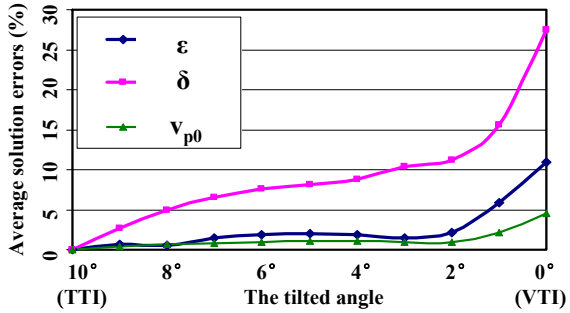

Figure 7: The influence of the tilted angle for the parameter estimation.

The sensitivity behaviors of TTI parameters will vary if the tilted angle is introduced. This example shows that the tilted angle has less effect on axial velocity and ε. It provides a feasible way to estimate the axial velocity and ε first if there is no information on the type of anisotropic media. When the tilted angle for the symmetry axis is assumed to be vertical (VTI) or inappropriate, such as normal to bedding, the estimation of δ will be unstable and degrade the quality of velocity model building.

We also analyze the influence of the layer thickness on the parameter estimation if given P-wave axial velocity. The true model is still same with Figure (4a) but we invert for ε, δ and the tilted angle φ. Two interfaces are adjusted toward shallower or deeper to test the influence of the layer thickness. The results illustrated in Figure 8 show that the thickness errors have less effect on the estimation of ε and φ. Therefore ε and φ can be treated as preferential inversion parameters if we have no other data information. Here, layer thickness error has a greater influence on the accuracy of estimating δ.

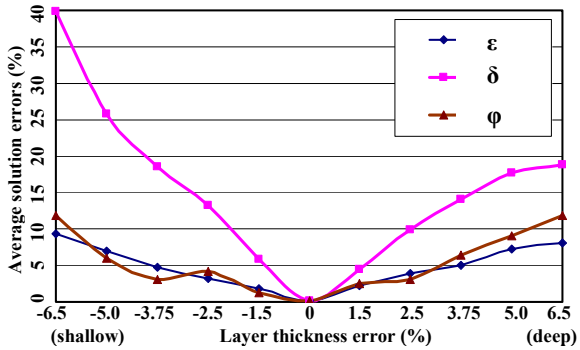

Figure 8: The influence of the layer thickness for the parameter estimation.

Based on above tests, a general workflow of TTI parameter estimation can be proposed as:

$$v_{p0} \Rightarrow \varepsilon \text{ or interface} \Rightarrow \varphi \text{ or interface} \Rightarrow \delta$$

Conclusions

We have developed a new 2D TTI first-arrival tomography method which works reasonably well in several synthetic tests. The analytical kernels derived illuminate the distinct sensitivity behaviours of individual TTI parameter. The tilted TI symmetry axis creates a new ambiguity in seismic tomography. Ignoring the tilted angle of symmetry axis by assuming it is vertical (VTI) or normal to bedding will degrade the quality of the parameter estimation. Our tests show that the error in estimating the symmetry angle and layer thickness in the presence of TTI may lead to significant distortions in image quality. A general workflow for TTI parameter estimation is proposed and to be tested with field data.

EDITED REFERENCES

Note: This reference list is a copy-edited version of the reference list submitted by the author. Reference lists for the 2009 SEG Technical Program Expanded Abstracts have been copy edited so that references provided with the online metadata for each paper will achieve a high degree of linking to cited sources that appear on the Web.

REFERENCES

Ball, G., 1995, Estimation of anisotropy and anisotropic 3-D prestack depth migration, offshore Zaire: Geophysics, **60**, 1495–1513.

Behera, L., and I. Tsvankin, 2009, Migration velocity analysis for tilted transversely isotropic media: Geophysical Prospecting, **57**, 13–26.

Charles, S., D. R. Mitchell, R. A. Holt, J. Lin, and J. Mathewson, 2008, Data-driven tomographic velocity analysis in tilted transversely isotropic media: A 3D case history from the Canadian Foothills: Geophysics, **73**, no. 5, VE261–VE268.

Grechka, V., A. Pech, I. Tsvankin, and B. Han, 2001, Velocity analysis for tilted transversely isotropic media: A physical modeling example: Geophysics, **66**, 904–910.

Hornby, B. E., L. M. Schwartz, and J. A. Hudson, 1994, Anisotropic effective-medium modeling of the elastic properties of shales: Geophysics, **59**, 1570–1583.

Koren, Z., I. Ravve, G. Gonzalez, and D. Kosloff, 2008, Anisotropic local tomography: Geophysics, **73**, no. 5, VE75–VE92.

Sayers, C. M., 2005, Seismic anisotropy of shales: Geophysical Prospecting, **53**, 667–676.

Sena, A. G., 1991, Seismic traveltime equations for azimuthally anisotropic and isotropic media: Estimation of interval elastic properties: Geophysics, **56**, 2090–2101.

Thomsen, L., 1986, Weak elastic anisotropy: Geophysics, **51**, 1954–1966.

———, 1995, Elastic anisotropy due to aligned cracks in porous rock: Geophysical Prospecting, **43**, 805–829.

Vestrum, R. W., D. C. Lawton, and R. Schmid, 1999, Imaging structures below dipping TI media: Geophysics, **64**, 1239–1246.

Zhou, B., S. A. Greenhalgh, and A. Green, 2008, Nonlinear traveltime inversion scheme for crosshole seismic tomography in tilted transversely isotropic media: Geophysics, **73**, no. 4, D17–D33.

Zhou, H., 2006, Multiscale deformable-layer tomography: Geophysics, **71**, no. 3, R11–R19.

Zhou, R., D. McAdow, C. Barberan, D. Dushman, and F. Doherty, 2004, Seismic anisotropy estimation in TTI media using walkaway VSP data: 74th Annual International Meeting, SEG, Expanded Abstracts, 2525–2528.